Improved performance of PtRu/C prepared by selective deposition of Ru on Pt as an anode for a polymer electrolyte membrane fuel cell

Hyun Tae Kim, Han-Ik Joh, Sang Heup Moon*

Department of Chemical & Biological Engineering and Institute of Chemical Processes, Seoul National University, San 56-1, Shillim-dong, Kwanak-ku, Seoul 151-744, Republic of Korea

ARTICLE INFO

ABSTRACT

Ru-promoted Pt/C catalysts with different Ru/Pt ratios are prepared by selective chemical vapour deposition (CVD) of Ru onto a Pt surface. The optimum PtRu/C (Ru/Pt = 0.44) catalyst prepared using a CVD method shows improved performance as an anode for a polymer electrolyte membrane fuel cell in the presence of CO, as compared with a commercial PtRu/C (Ru/Pt = 1) catalyst and a PtRu/C (Ru/Pt = 1) catalyst prepared using a conventional impregnation (IMP) method. This observation is confirmed by the results of half-cell and single-cell tests. The CVD catalyst shows an improved CO tolerance because Ru is preferentially deposited as nano-scale particles on the Pt surface and, consequently, the number of Pt particles that are in close contact with the added Ru is greater in the CVD catalyst. An increase in the interfacial area between the Ru and the Pt facilitates the transfer of the oxygen-containing species to the CO-poisoned Pt surface such that the oxidation of CO is promoted. The Pt surface is also modified electronically due to an interaction with the added Ru, which is stronger in the CVD catalyst than in the IMP catalyst, as demonstrated by X-ray photoelectron analysis.

1. Introduction

The fuel cell is widely recognized as an attractive device for obtaining electrical energy directly from chemicals. In particular, polymer electrolyte membrane fuel cells (PEMFCs) attracted attention due to the advantages of zero emission, rapid cell start-up and high specific power at low temperatures, generally at 60–100 °C [1–3]. For the successful commercialization of PEMFCs, however, some problems have to be resolved: most critically, carbon monoxide (CO) poisoning of the anode catalyst [4,5]. Even a small amount of CO in the fuel hydrogen will poison the Pt active sites and eventually degrade anode performance [6,7].

To solve this problem, researchers have studied bimetallic catalysts prepared by adding metals such as Ru, Rh, Sn, W and Mo to pure Pt [8–13]. Among the many Pt-based anodic catalysts thus far examined, the PtRu alloy catalyst has been the subject of most investigation, and the PtRu(Ru/Pt = 1)/C catalyst, in particular, has shown the highest CO tolerance.

Antolini and Cardellini [14] reported that the thermal treatment of PtRu/C in argon, which was prepared by a conventional impregnation (IMP) method, promoted the formation of an alloy in the catalyst, and that the Ru content of the alloy increased with increase in the treatment temperature due to the diffusion-controlled incorporation of Ru atoms into the Pt lattice. When, however, the PtRu/C catalyst was annealed at temperatures greater than a certain level, typically 700 °C, the enhanced interaction between the metal, Ru or Pt, and the support hindered the formation of the PtRu alloy. Consequently, only a limited fraction of the Ru (∼49%) alloyed with Pt. Furthermore, the high-temperature treatment caused sintering of the metal particles in the catalyst, thus reducing the metal surface area and, eventually, the catalyst activity.

As a possible solution to the above problem, Ru is added to a Pt/C catalyst in this study by means of a chemical vapour deposition (CVD) method, such that Ru is selectively deposited on the Pt surface instead of the carbon support. In this way, the added Ru is expected to interact more intimately with Pt and, consequently, the temperature required for the Pt–Ru alloy formation will be lowered from that required in the case of the IMP method [15,16].

The CO tolerance of the catalysts prepared by the CVD method is compared with catalysts prepared by the IMP method and with a commercial PtRu(Ru/Pt = 1)/C catalyst [17]. The performance of different catalysts is discussed based on the results of characterization studies with high-resolution transmission electron microscopy (HR-TEM), X-ray diffraction (XRD), and X-ray photoelectron spectroscopy (XPS).

* Corresponding author. Tel.: +82 2 880 7409; fax: +82 2 875 6697.
 E-mail address: shmoon@surf.snu.ac.kr (S.H. Moon).

2. Experimental

2.1. Preparation of PtRu/C catalysts

Prior to CVD experiments, a commercial 20 wt.% Pt/C catalyst (E-TEK Co.) was pre-reduced in a stream containing H_2 and N_2 at a ratio of 1:1 at 100 °C for 1 h. Then, the vapour of ruthenocene (ruthenium cyclopentadienyl, Aldrich), which was obtained by flowing nitrogen into a vessel holding the precursor at 170 °C, was introduced into a reactor containing the pre-reduced Pt/C catalyst, also maintained at 170 °C, together with hydrogen flowing at the same rate as nitrogen for 1 h. A reactor temperature of 170 °C was chosen for the CVD process because the results of separate thermogravimetric analysis (TGA) indicated that the Ru precursor vapourized slowly at 120 °C and rapidly at 220 °C.

After the Pt/C catalyst was treated in the CVD process, the partially decomposed ruthenocene, which remained on the catalyst, was eliminated from the surface by heating the catalyst at 220 °C in flowing hydrogen for 0.5 h. The catalyst was finally treated at different temperatures in flowing nitrogen for 0.5 h to allow the formation of a PtRu alloy. Meanwhile, the stream of the reactor was analyzed by FT-IR (Jasco, FT/IR-300E) during the above treatments. The Ru content of the final catalyst, which was controlled by the amount of Ru precursor introduced into the reactor, was measured by inductively coupled plasma–Auger electron spectroscopy (ICP–AES: Shimadzu, ICPS-1000IV). The catalyst prepared by the above CVD procedure is designated as Pt–xRu(C)y, where x and y indicate the Ru/Pt atomic ratio and the final treatment temperature (in units of °C), respectively. For the purpose of comparison, a PtRu(Ru/Pt = 1)/C catalyst was prepared by impregnating a commercial 20 wt.% Pt/C catalyst with $RuCl_3 \cdot H_2O$ (Aldrich), followed by reduction in hydrogen at 350 °C for 2.5 h. The catalyst is designated as Pt–1.0Ru(I)y in the same manner as the CVD catalyst.

2.2. Activity test

Electrodes for the CO-stripping measurements were prepared according to the method of Schmidt et al. [18]. An aqueous suspension of a sample catalyst, either a prepared PtRu catalyst or a commercial Pt–1.0Ru(E-TEK) catalyst, was prepared by dispersing the catalyst ultrasonically in pure water such that the suspension contained Pt at a level of 2 mg_{metal} ml^{-1}. The metal loading of the commercial catalyst was 20 wt.%, which included the amount of both Pt and Ru. Then, a 20 μl aliquot of the suspension was pipetted on to the glassy carbon substrate (6 mm dia., 0.283 cm^2), yielding a metal loading of ~7 mg_{metal} cm^{-2}. After the evaporation of the water droplets, 20 μl of a diluted Nafion solution (5 wt.%, Aldrich) was applied to the dried catalyst powder, and the solution was air-dried at room temperature. Finally, the electrode was immersed in deaerated 0.5 M H_2SO_4 electrolyte. Potentials were measured with respect to an Ag/AgCl reference electrode, but all potentials were referred to the standard hydrogen electrode scale (SHE). As the Nafion solution contained small amounts of contaminants, the electrode potential, which was controlled with a potentiostat (EG&G, M263), was applied in cycles between 0 and 650 mV to obtain clean electrode surfaces. For the CO-stripping measurements, the electrode potential was fixed at 0.1 V in CO-saturated electrolyte for 10 min and the potential scan, at a scan rate of 10 mV s^{-1}, was begun after CO had been completely purged from the electrolyte.

The single-cell performances of the prepared PtRu/C catalysts and the commercial catalyst were tested at 70 °C in a H_2/O_2 system at several CO concentrations. The membrane-electrode assemblies (MEAs) used Nafion 212 (Dupont) as a polymer electrolyte. Either prepared PtRu/C catalysts or a commercial 20 wt.% PtRu/C with a Ru/Pt ratio of 1 was used as an anode and a commercial 40 wt.% Pt/C(E-TEK) was used as a cathode for single-cell tests. The cata-
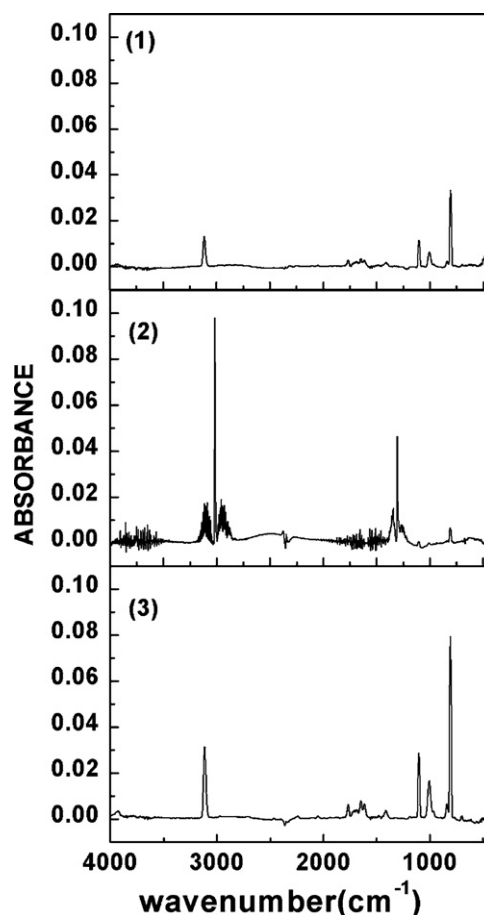

Fig. 1. FT-IR spectrum of gas stream at exit of reactor containing (1) carbon or (2) Pt/C, or from (3) blank reactor. Feed = ruthenocene; temp. = 170 °C.

lyst loading in the anode and the cathode was 0.25 mg_{Pt} cm^{-2} and 0.3 mg_{Pt} cm^{-2}, respectively. The single-cell with an active area of 5 cm^2 was fed with 200 ml min^{-1} of H_2, either pure or containing CO at various concentrations, at the anode and with 200 ml min^{-1} of pure O_2 at the cathode.

2.3. Characterization of catalysts

High-resolution transmission electron microscopy (HR-TEM: JEOL JEM-3010) and energy-dispersive X-ray spectroscopy (EDX: Oxford, QX-2000) attached to the HR-TEM were used to confirm the selective deposition of Ru on the Pt surface.

The degree of Pt–Ru alloy formation was estimated by X-ray diffraction (XRD: Rigaku, 12kw-XRD) using Cu Kα (λ = 1.5405 Å) analysis. The XRD peaks were assigned based on the database of the Joint Committee on Powder Diffraction Standards (JCPDS), and the lattice parameter was determined for Pt(2 2 0).

The binding energies of Pt 4f electrons were obtained from X-ray photoelectron spectra (XPS: Sigma Probe, ThermoVG, UK), measured using an Mg X-ray (1486.6 eV) source, and were calibrated with C 1s (284.5 eV).

3. Results and discussion

3.1. Selective deposition of Ru on Pt

Fig. 1 shows the FT-IR spectra of the reactor exit streams, which were obtained after ruthenocene vapour had been introduced into a reactor containing either (1) carbon or (2) the pre-reduced Pt/C

and after the reactor had been subsequently flushed with an $H_2–N_2$ mixture. The spectrum of a stream from a blank reactor, (3) was also obtained for comparison. The spectrum obtained from a reactor containing the carbon support, (1) is the same as that from a blank reactor, (3) except for a slight decrease in the overall peak intensity. The observation of a ring-tilt peak at ca. 450 cm^{-1}, representing the bond between Ru and the cyclopentadienyl ligand, for (1) indicates that ruthenocene is not decomposed on the carbon. On the other hand, when the reactor contained the pre-reduced Pt/C, (2) the intensity of the ring-tilt peak is decreased significantly and new peaks appear at about 1300 cm^{-1} and 3000 cm^{-1}, which indicates that ruthenocene is decomposed due to the reaction between the cyclopentadienyl ligand and hydrogen adsorbed on the Pt surface [19,20].

To examine further the selective deposition of Ru on the Pt surface instead of on the carbon, the line profile of Pt–0.44Ru(C)600 was analyzed by EDX attached to HR-TEM (Fig. 2). The reason why the catalyst was treated at 600 °C is explained later in Section 3.2. Line (a) in Fig. 2 indicates the position of the sample that was analyzed by EDX, and the peaks of red and sky-blue colours represent the detected Pt and Ru, respectively (For interpretation of the references to colour in this sentence, the reader is referred to the web version of the article.). It is apparent from the results that the majority of the Ru species are in close proximity to the Pt particles.

Table 1 lists the Ru/Pt atomic ratios estimated from the EDX analyses of particles that were randomly selected on the surfaces of two sample catalysts (Fig. 3). Although the data are scattered
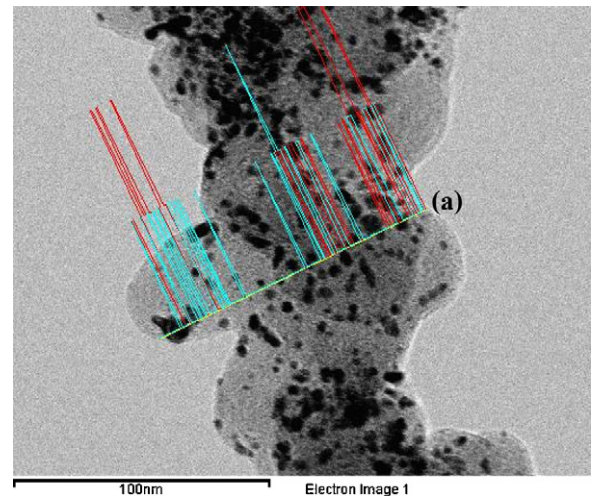

Fig. 2. Line profile results of Pt–0.44Ru(C)600 analyzed by EDX attached to HR-TEM.

due to errors involved in the analyses, the scattering is greater for Pt–1.0Ru(I)600 than for Pt–0.44Ru(C)600. In the case of the former catalyst, the Ru is nearly undetectable in particles (1) and (2) (Fig. 3(a)), but the amount detected in particle (3) is 30 times greater than that in particle (4) (Fig. 3(b)). In addition, the average Ru/Pt ratio obtained from the above data significantly deviates from
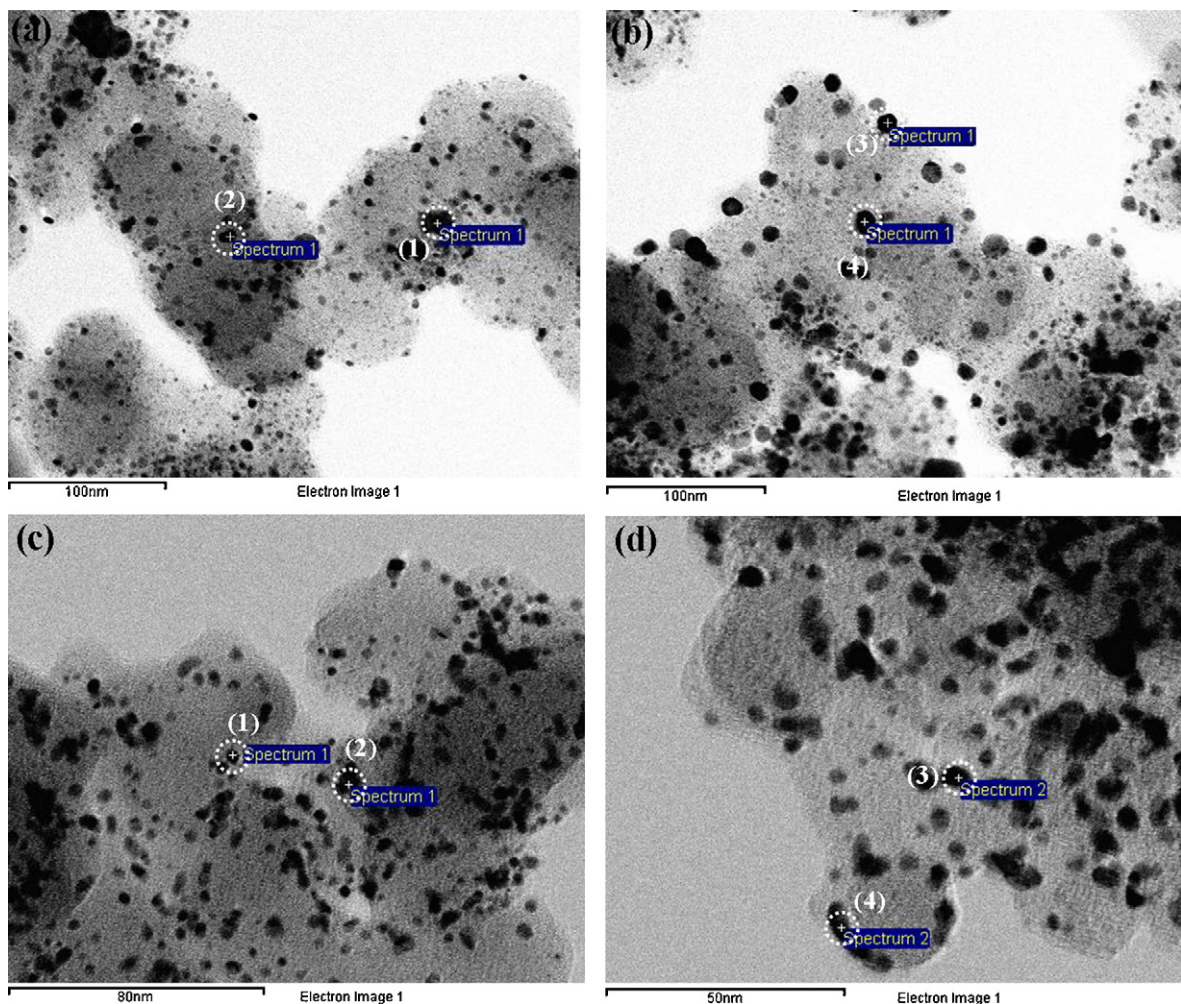

Fig. 3. Point analysis of PtRu catalysts. (a and b) Pt–1.0Ru(I)600; (c and d) Pt–0.44Ru(C)600.

Table 1
Ru:Pt atomic ratios calculated by ICP–AES and EDX analysis.

Pt–1.0Ru(I)600			Pt–0.44Ru(C)600		
ICP–AES	EDX		ICP–AES	EDX	
	Point (1)	0.1		Point (1)	0.52
	Point (2)	0.0		Point (2)	0.42
1.0	Point (3)	39	0.44	Point (3)	0.71
	Point (4)	1.3		Point (4)	0.13
	Average	10		Average	0.45

the value estimated by ICP–AES. On the other hand, the data from Pt–0.44Ru(C)600 are scattered to smaller extents, i.e., between 0.13 and 0.71, and the average Ru/Pt ratio is similar to the ICP–AES value. Accordingly, it is concluded that the Ru added by CVD is preferentially deposited on the Pt surface, whereas the Ru added by IMP is randomly distributed on the catalyst surface.

3.2. Conditions for an optimum catalyst

Table 2 lists two sets of Ru contents for the sample catalysts: (a) the nominal Ru/Pt atomic ratios obtained by assuming that the ruthenocene introduced into the CVD reactor is completely decomposed and deposited on the catalyst surface, and (b) the actual Ru/Pt ratios obtained from ICP–AES analysis of the catalysts. The actual Ru/Pt ratios are slightly lower than the nominal ones, but both sets of data change in parallel. It is noteworthy that the actual Ru/Pt ratios of many catalysts exceed 0.3, which is the measured Pt dispersion of the Pt/C catalyst prior to Ru addition and, therefore, should be a limit to the Ru:Pt ratio if the deposited Ru forms a maximum monolayer on the Pt surface. Excessive deposition of Ru is possible when Ru atoms are either incorporated into the lattice of the Pt particles or deposited on the Pt surface as multilayers. Between the two options, the former is not likely because the temperature of the CVD process, viz., 170 °C, is too low to decompose completely the Ru precursor in the catalysts. This proposition is confirmed by temperature-programmed-reduction (TPR) of the catalyst, although the results are not shown here. Consequently, the formation of Pt–Ru alloys [21,22] in the catalysts is retarded due to cyclopentadienyl ligands remaining in the catalysts. On the other hand, the mulilayer deposition of Ru may well occur because hydrogen can be dissociatively adsorbed on the surface of the deposited Ru [23] such that rucenothene is additionally decomposed on the Ru surface to form multilayers.

The prepared catalysts with different Ru contents were tested for CO-stripping to determine the optimum Ru/Pt atomic ratio required for maximizing the effect of Ru as a promoter. Fig. 4 shows the measured current–voltage (CV) curves and the CO oxidation potentials obtained from the CV results. The CO oxidation potential initially decreases with increase in the Ru/Pt ratio, but eventually increases at ratios higher than the optimum value of 0.44. This optimum value for the catalyst prepared by Ru-CVD is lower than ~1.0, which is commonly required for maximizing the CO tolerance of PtRu/C catalysts prepared using the IMP method [24–26].

Table 2
(a) Nominal Ru:Pt atomic ratios and (b) Ru:Pt atomic ratios calculated using ICP–AES results of catalysts prepared by CVD of Ru.

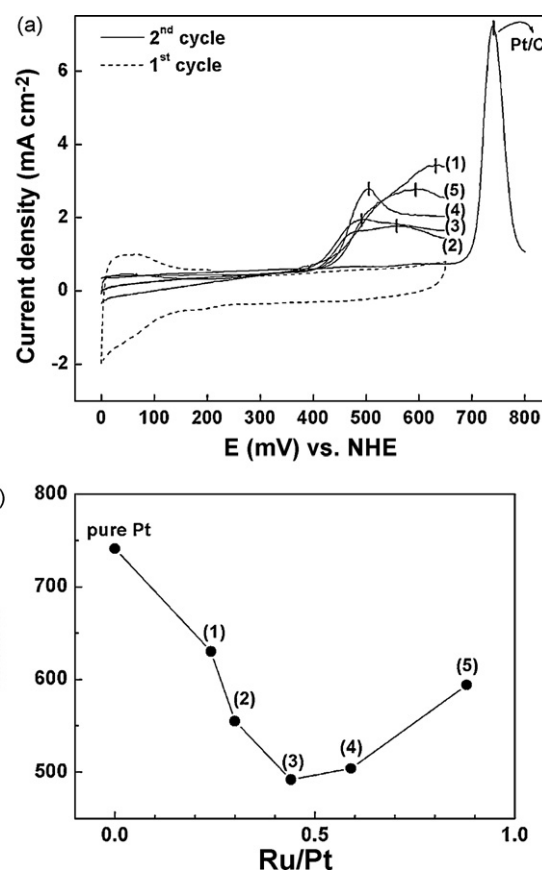| Sample	Ru:Pt	
	(a) Nominal value	(b) ICP–AES
Pt–0.24Ru(C)	0.25	0.24
Pt–0.30Ru(C)	0.33	0.30
Pt–0.44Ru(C)	0.50	0.44
Pt–0.59Ru(C)	0.66	0.59
Pt–0.88Ru(C)	1.00	0.88

Fig. 4. (a) Results of CO-stripping test, and (b) CO oxidation potentials obtained using catalysts with different Ru contents: (1) Pt–0.24Ru(C); (2) Pt–0.30Ru(C); (3) Pt–0.44Ru(C); (4) Pt–0.59Ru(C); (5) Pt–0.88Ru(C).

In the XRD patterns of the catalysts, the peak associated with a Pt(1 1 1) plane gradually shifts to higher angles with increase in the Ru content (Fig. 5). These results indicate a decrease in the lattice constant in the presence of Ru that corresponds to the formation of a PtRu alloy [11]. Antolini and Cardellini [14] reported that PtRu/C catalysts prepared by the IMP method began to form a Pt–Ru alloy when they were treated at 300 °C in Ar. In the present study, the alloy was formed at a lower temperature, 220 °C, which suggests
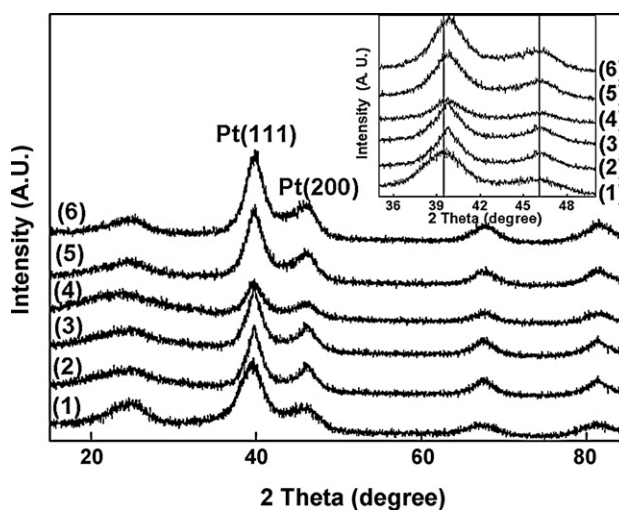

Fig. 5. XRD patterns of PtRu:C catalysts containing different amounts of Ru added by CVD: (1) 20 wt.% Pt/C; (2) Pt–0.24Ru(C); (3) Pt–0.30Ru(C); (4) Pt–0.44Ru(C); (5) Pt–0.59Ru(C); (6) Pt–0.88Ru(C).
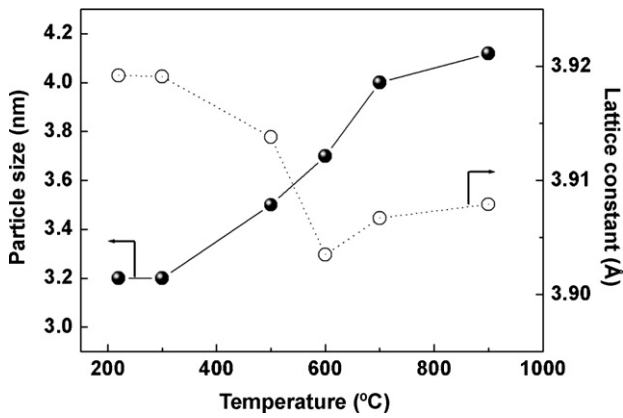
Fig. 6. Changes in particle size and the lattice constant of Pt–0.44Ru(C) with annealing temperature.

Fig. 7. Results of CO-stripping tests showing CO oxidation potential of (1) Pt–1.0Ru(I)600, (2) Pt–1.0Ru(I)700, (3) Pt–0.44Ru(C)600, and (4) commercial Pt–1.0Ru(E-TEK).

that the Ru added by CVD interacts more intimately with the Pt surface than when Ru is added by IMP.

The Pt–0.44Ru(C) catalyst was treated in flowing N_2 at different temperatures to determine the optimal temperature for Pt–Ru alloy formation. Changes in the average particle size and the lattice constant of the Pt, as estimated from the XRD patterns at different temperatures, are presented in Fig. 6. The Pt particle size consistently increases with increase in temperature. On the other hand, the lattice constant initially decreases with increasing temperature, reaches a minimum at approximately 600 °C, and becomes nearly constant at higher temperatures (above 700 °C). The initial decrease in the lattice constant is due to the formation of an alloy between Pt and Ru, the latter has an atomic radius that is smaller than the former [27]. Alloy formation is inhibited at temperatures above 700 °C because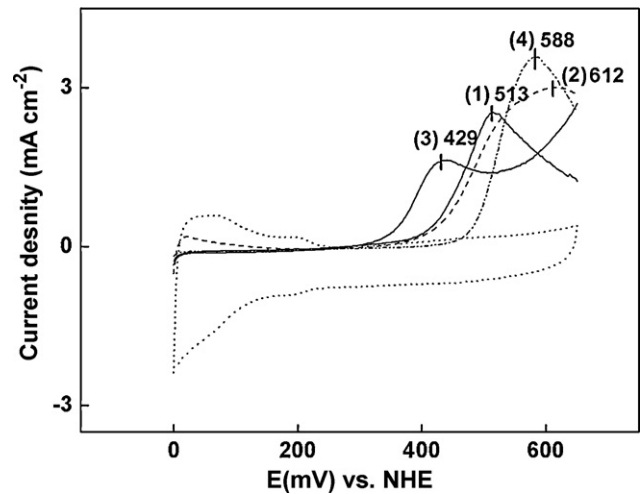 Pt starts to interact with the C support, as reported previously [28]. Consequently, the optimum temperature for Pt–Ru alloy formation in Pt–0.44Ru(C) is determined to be 600 °C.

3.3. Comparison of catalyst performance

The CO oxidation potentials of four sample catalysts, namely, Pt–0.44Ru(C)600, Pt–1.0Ru(I)600, Pt–1.0Ru(I)700 and a commercial Pt–1.0Ru(E-TEK), are given in Fig. 7. Two Pt–1.0Ru(I) catalysts were tested, i.e., after treatment at 600 and 700 °C, to determine the proper temperature for treating the catalyst. Pt–1.0Ru(I)600 shows a lower potential, 513 mV, than that of Pt–1.0Ru(I)700, 612 mV,
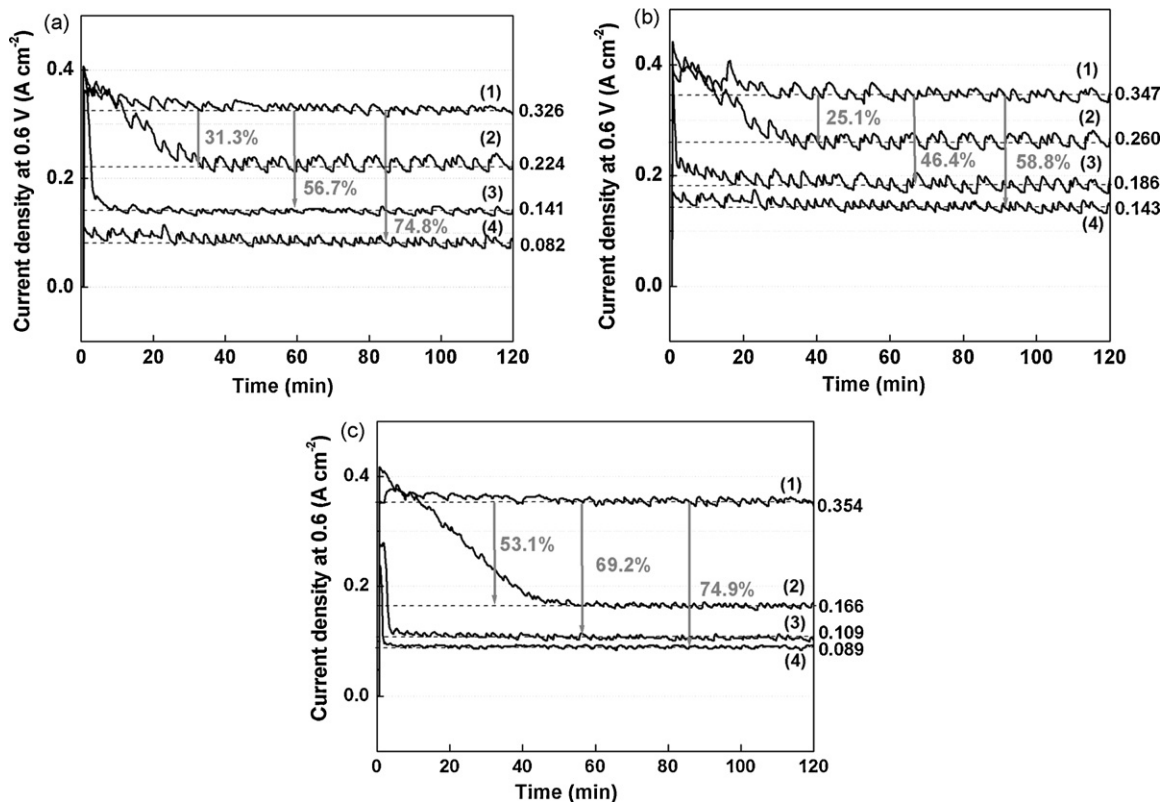

Fig. 8. Single-cell performance at 0.6 V for (a) Pt–1.0Ru(I)600, (b) Pt–0.44Ru(C)600, and (c) Pt–1.0Ru(E-TEK) for 2 h at several CO concentrations: (1) pure H_2; (2) 10 ppm; (3) 50 ppm; (4) 100 ppm.
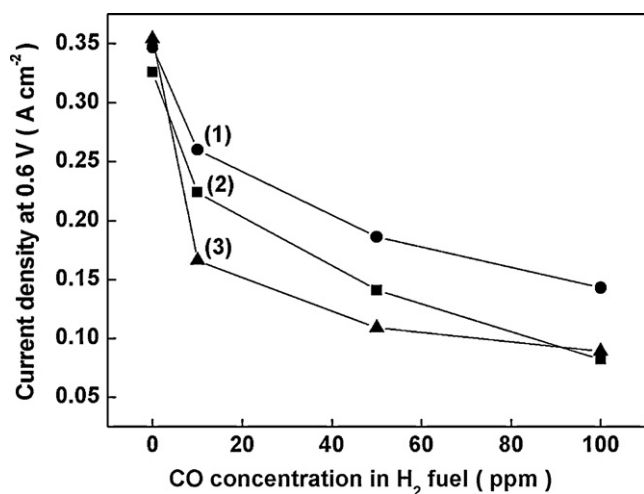
Fig. 9. Performance degradation plots for (1) Pt–0.44Ru(C)600, (2) Pt–1.0Ru(I)600, and (3) Pt–1.0Ru(E-TEK) as function of CO concentrations.

because Pt–Ru alloy formation is hindered due to an interaction between the metal, Pt or Ru, and C at 700 °C [14]. Among the tested catalysts, Pt–0.44Ru(C)600 gives the best performance with the lowest CO oxidation potential, at 429 mV.

The CO tolerance of the catalysts, excluding Pt–1.0Ru(I)700, was also examined at different CO partial pressures by single-cell tests, as shown in Figs. 8 and 9. The performance of all catalysts is degraded when the anodic fuel contains CO. In particular, the commercial PtRu/C catalyst experiences a significant decrease in current density even at a low partial pressure of CO, viz., 10 ppm, compared with prepared catalysts. Pt–1.0Ru(I)600 gives current densities higher than those from commercial catalyst at CO pressures of 10 and 50 ppm, but the performance of the two catalysts becomes similar at a CO pressure of 100 ppm. On the other hand, Pt–0.44Ru(C)600 consistently delivers higher current densities than for the other two catalysts at all CO pressures.

3.4. Origin of improved performance of Pt–0.44Ru(C)600

The role of Ru in promoting the CO tolerance of the Pt catalyst as an anode in a PEMFC has been attributed to two mechanisms [21]. One is a bifunctional mechanism, which suggests that the oxygen-

Fig. 10. XPS of Pt 4f in (1) Pt alone, (2) Pt–1.0Ru(I)600, and (3) Pt–0.44Ru(C)600.

containing species adsorbed on the Ru migrates to the Pt surface to facilitate the oxidation of CO on Pt [29]. The other mechanism is the electronic modification of Pt by interaction with the added Ru, i.e., Pt–Ru alloy formation, that lowers the potential for CO oxidation on Pt [30].

The present study demonstrates, from IR (Fig. 1) and EDX (Figs. 2 and 3) results, that Ru added by CVD is present close to the Pt surface and should facilitate the transfer of oxygen-containing species from Ru to Pt and, therefore, promotes the oxidation of CO on Pt. X-ray diffraction results (Fig. 4) show a shift in the Pt(1 1 1) peak to higher angles with an increase in the amount of Ru added by CVD, and thereby suggests the formation of a Pt–Ru alloy when the catalyst is treated at a temperature as low as 220 °C.

To investigate further the efficiency of the CVD method for promoting alloy formation compared with the IMP method, XPS of Pt is compared for three catalysts, namely, Pt/C, Pt–1.0Ru(I)600 and Pt–0.44Ru(C)600. In Fig. 10, the Pt peaks shift to lower binding energies due to Ru addition, which indicates the migration of electrons from Ru to Pt in accordance with the previous studies [31,32]. The binding energy shift is larger in Pt–0.44Ru(C)600 than in Pt–1.0Ru(I)600, supporting the contention that Pt is modified by Ru to a greater extent when the latter is added by CVD rather than by IMP.

Accordingly, it is concluded that Ru added by CVD is more efficient in promoting the Pt/C catalyst than that added by IMP because the former Ru is selectively deposited on and more closely interacts with the Pt surface, and thereby contributes to two mechanisms of catalyst promotion.

4. Conclusions

This study demonstrates that the CO tolerance of a Pt–Ru/C catalyst as an anode for a PEMFC is improved when Ru is added to Pt/C by CVD rather than by IMP. The Ru content required for optimum catalyst performance is lower in the former case than in the latter. These results are obtained because Ru is preferentially deposited on the Pt surface by CVD, and thereby facilitates both geometric and electronic interactions between Ru and the Pt. The deposition of Ru on the Pt and the close proximity between the Ru and Pt components are confirmed by FT-IR and EDX analyses. Alloy formation and electronic interactions between Pt and Ru are demonstrated by XRD and XPS analysis.

Pt–0.44Ru(C)600, which is prepared under conditions that will optimize the performance of the Pt–Ru(C) catalysts, exhibits the lowest CO oxidation potential and the highest CO tolerance among the sample catalysts, including one containing Ru added by IMP, Pt–1.0Ru(I)600, and a commercial catalyst, Pt–1.0Ru(E-TEK).

References

[1] S.J. Lee, S. Mukerjee, E.A. Ticianelli, J. McBreen, Electrochim. Acta 44 (1999) 3283–3293.
[2] E. Antolini, Mater. Chem. Phys. 78 (2003) 563–573.
[3] J.-H. Wee, K.-Y. Lee, J. Power Sources 157 (2006) 128–135.
[4] J. Divisek, H.F. Oetjen, V. Peinecke, V.M. Schmidt, U. Stimming, Electrochim. Acta 43 (1998) 3811–3815.
[5] D. Lee, S. Hwang, I. Lee, J. Power Sources 145 (2005) 147–153.
[6] A. Manasilp, E. Gulari, Appl. Catal. B 37 (2002) 17–25.
[7] R. Parsons, T. VanderNoot, J. Electroanal. Chem. 257 (1988) 9–45.
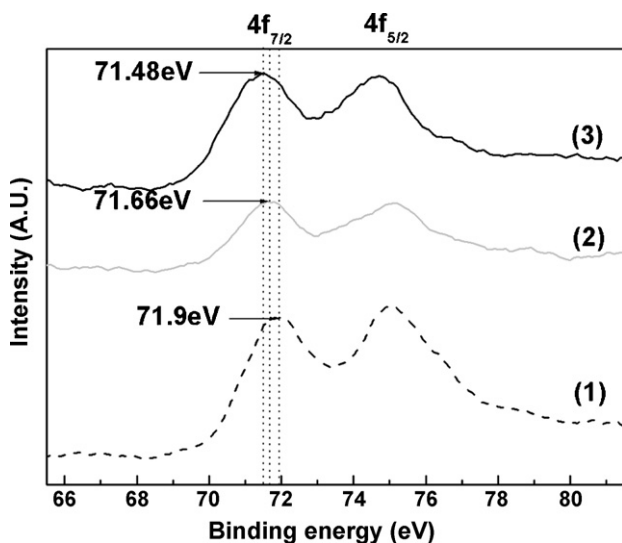[8] G. Avgouropoulos, T. Ioannides, Appl. Catal. B 56 (2005) 77–86.

[9] B. Beden, C. Lamy, N.R. de Tacconi, A.J. Arvia, Electrochim. Acta 35 (1990) 691–704.
[10] M. Gotz, H. Wendt, Electrochim. Acta 43 (1998) 3637–3644.
[11] L. Giorgi, A. Pozio, C. Bracchini, R. Giorgi, S. Turtu, J. Appl. Electrochem. 31 (2001) 325–334.
[12] M. Arenz, V. Stamenkovic, B.B. Blizanac, K.J. Mayrhofer, N.M. Markovic, P.N. Ross, J. Catal. 232 (2005) 402–410.
[13] J.G. Wang, B. Hammer, J. Catal. 243 (2006) 192–198.
[14] E. Antolini, F. Cardellini, J. Alloys Compd. 315 (2001) 118–122.
[15] S.J. Seo, H.-I. Joh, H.T. Kim, S.H. Moon, Electrochim. Acta 52 (2006) 1676–1682.
[16] S.J. Seo, H.-I. Joh, H.T. Kim, S.H. Moon, J. Power Sources 163 (2006) 403–408.
[17] A. Hamnett, Catal. Today 38 (1997) 445–457.
[18] T.J. Schmidt, H.A. Gasteiger, G.D. Stab, P.M. Urban, D.M. Kolb, R.J. Behm, J. Electrochem. Soc. 145 (1998) 2354–2358.
[19] H. Miura, Catal. Today 28 (1996) 215–221.
[20] J.S. Bodenheimer, W. Low, Spectrochim. Acta A 29 (1973) 1733–1743.
[21] M.T.M. Koper, Surf. Sci. 548 (2004) 1–3.
[22] H. Rauscher, T. Hager, T. Diemant, H. Hoster, F. Buatier de Mongeot, R.J. Behm, Surf. Sci. 601 (2007) 4608–4619.
[23] A. Onda, T. Komatsu, T. Yashima, J. Catal. 201 (2001) 13–21.
[24] H.A. Gasteiger, N. Markovic, P.N. Ross, E.J. Cairns, J. Phys. Chem. A 98 (1994) 617–625.
[25] H.A. Gasteiger, N.M. Markovic, P.N. Ross, J. Phys. Chem. A 99 (1995) 8290–8301.
[26] W.F. Lin, M.S. Zei, M. Eiswirth, G. Ertl, T. Iwasita, W. Vielstich, J. Phys. Chem. B 103 (1999) 6968–6977.
[27] T.F. Fuller, F.J. Luczak, D.J. Wheeler, J. Electrochem. Soc. 142 (1995) 1752–1757.
[28] E. Antolini, J. Power Sources 170 (2007) 1–12.
[29] E. Ticanelli, J.G. Beery, M.T. Paffett, S. Gottesfeld, J. Electroanal. Chem. 258 (1989) 61–77.
[30] M. Watanabe, S. Motoo, J. Electroanal. Chem. 60 (1975) 275–283.
[31] M.C. Denis, G. Lalande, D. Guay, J.P. Dodelet, R. Schulz, J. Appl. Electrochem. 29 (1999) 951–960.
[32] J.B. Goodenough, R. Manoharan, A.K. Shukla, K.V. Ramesh, Chem. Mater. 1 (1989) 391–398.